







Research Article

Sepsis shapes the human $\gamma\delta$ TCR repertoire in an age- and pathogen-dependent manner

Eric Giannoni^{*1} , Guillem Sanchez Sanchez^{*2,3,4,5} , Isoline Verdebout^{2,3,4,5},
Maria Papadopoulou^{2,3,4,5} , Moosa Rezvani^{2,3,4,5} , Raya Ahmed⁶, Kristin Ladell^{6,7},
Kelly L. Miners⁶, James E. McLaren^{6,7}, Donald J. Fraser^{6,7,8,9}, David A. Price^{6,7},
Matthias Eberl^{6,7} , Swiss Pediatric Sepsis Study, Philipp K.A. Agyeman¹⁰,
Luregn J Schlapbach^{11,12} and David Vermijlen^{2,3,4,5} 

¹ Clinic of Neonatology, Department Mother-Woman-Child, Lausanne University Hospital and University of Lausanne, Lausanne, Switzerland

² Department of Pharmacotherapy and Pharmaceutics, Université Libre de Bruxelles (ULB), Brussels, Belgium

³ Institute for Medical Immunology (IMI), Université Libre de Bruxelles (ULB), Brussels, Belgium

⁴ ULB Center for Research in Immunology (U-CRI), Université Libre de Bruxelles (ULB), Brussels, Belgium

⁵ WELBIO Department, WEL Research Institute, Wavre, Belgium

⁶ Division of Infection and Immunity, School of Medicine, Cardiff University, Cardiff, UK

⁷ Systems Immunity Research Institute, Cardiff University, Cardiff, UK

⁸ Wales Kidney Research Unit, Heath Park Campus, Cardiff, UK

⁹ Directorate of Nephrology and Transplantation, Cardiff and Vale University Health Board, University Hospital of Wales, Cardiff, UK

¹⁰ Department of Pediatrics, Inselspital, Bern University Hospital/University of Bern, Bern, Switzerland

¹¹ Department of Intensive Care and Neonatology, and Children's Research Center, University Children's Hospital Zurich, Zurich, Switzerland

¹² Child Health Research Centre, University of Queensland, Brisbane, Australia

Sepsis affects 25 million children per year globally, leading to 2.9 million deaths and substantial disability in survivors. Extensive characterization of interactions between the host and bacteria in children is required to design novel preventive and therapeutic strategies tailored to this age group. $V\gamma9V\delta2$ T cells are the first T cells generated in humans. These cells are defined by the expression of $V\gamma9V\delta2$ T-cell receptors (TCRs, using the TRGV9 and TRDV2 gene segments), which react strongly against the prototypical bacterial phosphoantigen HMBPP. We investigated this reactivity by analyzing the TCR δ (TRD) repertoire in the blood of 76 children (0–16 years) with blood culture-proven bacterial sepsis caused by HMBPP-positive *Escherichia coli* or by HMBPP-negative *Staphylococcus aureus* or by HMBPP-negative *Streptococcus pneumoniae*. Strikingly, we found that *S. aureus*, and to a lesser extent *E. coli* but not *S. pneumoniae*, shaped the TRDV2 repertoire in young children (<2 years) but not in older children or adults. This dichotomy was due to the selective expansion of a fetal TRDV2 repertoire. Thus, young children possess fetal-derived $V\gamma9V\delta2$ T cells that are highly responsive toward specific bacterial pathogens.

Keywords: $\gamma\delta$ T cells · Neonate immunity · TCR · Sepsis



Additional supporting information may be found online in the Supporting Information section at the end of the article.

Correspondence: Prof. David Vermijlen
e-mail: david.vermijlen@ulb.be

*These authors contributed equally to the work.

Introduction

Sepsis contributes to a major burden of disease in early life. Worldwide, it is estimated that half of the 48.9 million annual cases of sepsis occur in children, leading to 2.9 million deaths [1]. This vulnerability in early life is not unexpected, given the predominantly naïve phenotype of neonatal immune cells and distinctive immunological challenges at birth and during childhood [2–4]. Attempts at modulating the immune system of newborns and young children to prevent or treat infections have yielded only limited benefits to date [3]. Therefore, extensive characterization of host–pathogen interactions in early life is required to develop novel preventive and therapeutic strategies [3].

$\gamma\delta$ T cells express T-cell receptors (TCRs), each comprising a TRG (γ) and TRD (δ) chain, and are not restricted by classical MHC molecules, unlike conventional $\alpha\beta$ T cells expressing $\alpha\beta$ TCRs [5, 6]. Somatic rearrangements of the TRG and TRD loci take place during the development of $\gamma\delta$ T cells from a common $\alpha\beta/\gamma\delta$ T-cell precursor in the thymus, where variable (V), diversity (D, only for TRD), and joining (J) gene segments are used to form each a complete γ and δ chain, respectively [7]. The variability created during the V(D)J recombination is significantly enhanced by the junctional diversity, which includes the introduction of random nucleotides (N additions), a process mediated by the enzyme terminal deoxynucleotidyl transferase (TdT). The most variable domain, which includes these N additions and is usually accountable for antigen recognition, is termed the complementarity determining region 3 (CDR3) [8]. $\gamma\delta$ T cells have been implicated in a wide range of immunological scenarios in health and disease, including bacterial and viral infections [5, 9]. In humans, $\gamma\delta$ T cells can be divided into the innate-like phosphoantigen-reactive $V\gamma9V\delta2$ T cells (V gene segments of the γ and δ chains encoded by TRGV9 and TRDV2 gene segments, respectively), and the more adaptive-like non- $V\gamma9V\delta2$ $\gamma\delta$ T cells (e.g. $V\delta1^+$ $\gamma\delta$ T cells) that can potentially react to a variety of antigen/ligand types [9–11]. “Phosphoantigens” are small phosphorus-containing molecules epitomized by the prototypical compound (*E*)-4-hydroxy-3-methyl-but-2-enyl pyrophosphate (HMBPP) [12–14]. HMBPP is generated in the 2-C-methyl-D-erythritol 4-phosphate (MEP) pathway of isoprenoid synthesis that is present in many bacteria but not in human cells [12]. As the biological activity of HMBPP is approximately 10,000 higher than that of the ubiquitous phosphoantigen isopentenyl pyrophosphate (IPP), the end product of both the MEP and the mevalonate pathway of isoprenoid synthesis, $V\gamma9V\delta2$ T cells are thought to detect bacterial infections primarily via HMBPP [12, 14]. Of note, despite the innate-like reactivity of $V\gamma9V\delta2$ T cells, the corresponding TRDV2-containing CDR3 repertoire is highly variable and it is not clear whether particular TRDV2-containing TCRs are more responsive than others toward particular infections [15].

$\gamma\delta$ T cells are the first T cells generated in the vast majority of vertebrate species, including humans. During this early life period, they show a distinct thymic development compared with their counterparts in adults and can play an important role in viral and parasitic infection in early life [8, 16–29]. However, it is not

clear whether $V\gamma9V\delta2$ T cells can react to invasive bacterial infection in children [23, 30–32]. As mice do not have $V\gamma9V\delta2$ T cells [33], studying the role of these cells in vivo requires well-designed human cohorts. Here, we used high-throughput sequencing of the TRD repertoire to examine how $V\gamma9V\delta2$ T cells respond in children with blood culture-proven sepsis. We focused on HMBPP-positive *Escherichia coli*, HMBPP-negative *Staphylococcus aureus*, and HMBPP-negative *Streptococcus pneumoniae*, which are major pathogens of sepsis in children [34, 35].

Strikingly, we found a substantial expansion of fetal-derived TRDV2 repertoire in children younger than two years infected with HMBPP-negative *S. aureus*, and, to a lesser extent, in children infected with HMBPP-positive *E. coli*. In contrast, infection with HMBPP-negative *S. pneumoniae* did not affect the TRDV2 repertoire. Children older than 2 years and adults infected with *S. aureus* or *E. coli* did not show these fetal-derived $V\gamma9V\delta2$ T-cell expansions. Accordingly, the distinct thymic development of $V\gamma9V\delta2$ T cells in the human fetus appears to have important functional consequences for the cellular immune response against invasive bacterial infections in early childhood.

Results

Patient characteristics

We analyzed the TRD repertoire in the blood of 76 children with blood culture-proven sepsis caused by *S. pneumoniae* ($n = 20$), *S. aureus* ($n = 36$), and *E. coli* ($n = 20$) (Table 1). The median postnatal age at sepsis onset was 48 months (IQR 20–82), 104 months (IQR 15–141), and 14 months (IQR 2–82) in *S. pneumoniae*, *S. aureus*, and *E. coli* sepsis, respectively (Table 1; Supporting Information Fig. S1). The proportion of patients with organ dysfunction during the course of infection was 35% (7/20), 31% (11/36), and 40% (8/20) for cases of *S. pneumoniae*, *S. aureus*, and *E. coli* sepsis, respectively (Table 1). None of the patients died. The median time between sepsis onset and sampling for analysis of the TRD repertoire via high throughput sequencing was similar across the different pathogen groups, with a median of 3–4 days (Table 1).

The TRD repertoire in children changes upon aging

Given the well-known impact of age on the development and function of many components of the immune system [36–39], we assessed the relationship between age and the TRD repertoire in children with blood culture-proven sepsis, distinguishing the etiologic agents *E. coli*, *S. aureus*, and *S. pneumoniae*. No clear differences in the occurrence of TRDV2 and TRDV1 gene segments were observed according to pathogen (Fig. 1A), but there was a common increase in the number of N additions among the TRDV2-containing CDR3 sequences, reaching almost 10 N additions at the age of 16 years (Fig. 1B, left panel). In contrast, the number of N additions among the TRDV1-containing CDR3

Table 1. Baseline demographics and clinical characteristics of children with blood culture-proven sepsis.

	All sepsis cases (n = 76)	Streptococcus pneumoniae (n = 20)	Staphylococcus aureus (n = 36)	Escherichia coli (n = 20)	p-value ^a
Female sex	26 (34%)	5 (25%)	11 (31%)	10 (50%)	0.20
Age at sepsis, months	52 (9–126)	48 (20–82)	104 (15–141)	14 (2–82)	0.02
Comorbidity present ^b	26 (34%)	0	15 (42%)	11 (55%)	<0.001
Site of infection					<0.001
Pneumonia	16 (21%)	12 (60%)	4 (11%)	0	
Osteoarticular	14 (18%)	1 (5%)	13 (36%)	0	
Urinary tract	13 (17%)	0	1 (3%)	12 (60%)	
Central nervous system	8 (11%)	6 (30%)	0	2 (10%)	
Skin and soft tissue	8 (11%)	0	8 (22%)	0	
Other specific infection types ^c	3 (4%)	0	3 (8%)	0	
Admission to an intensive care unit	24 (32%)	9 (45%)	10 (28%)	5 (25%)	0.32
Number of organ dysfunctions ^d					0.04
0	50 (66%)	13 (65%)	25 (69%)	12 (60%)	
1	12 (16%)	1 (5%)	5 (14%)	6 (30%)	
>1	14 (18%)	6 (30%)	6 (17%)	2 (10%)	
Timing of sampling, days ^e	3 (2–6)	3 (3–6)	3 (3–5)	3 (2–5)	0.46

Note: Categorical variables are presented as frequencies (%), and continuous variables as median (interquartile range).

^a p-value from Fisher's exact test for categorical variables and analysis of variance for continuous variables.

^b Defined by the presence of chronic congenital or acquired medical conditions.

^c Endocarditis and myositis.

^d Defined according to reference #68.

^e Number of days between sepsis onset and blood sampling for RNA analysis.

sequences was already at higher levels just after birth (mean of 15 N additions), as observed previously in cord blood [29, 40], and remained stable until the age of 16 years (Fig. 1B, right panel). Similarly, TRDJ3 use among TRDV2-containing CDR3 sequences was common early after birth, as reported previously [29, 40, 41], and declined steadily with age, whereas the opposite trend was observed for TRDJ1 (Fig. 1C). Thus, the TRD repertoire obtained from whole blood TRD sequencing in our pediatric sepsis cohort is consistent with previous observations on sorted $\gamma\delta$ T cells [29, 40, 41]. Principal component analysis (PCA) of multiple TRD characteristics versus age identified two clusters, segregated as children aged <2 years and children aged \geq 2 years (Supporting Information Fig. S1B and C; Fig. 1D). Subsequent analyses were conducted on the basis that young children (<2 years) might have different $\gamma\delta$ T-cell responses than older children (\geq 2 years).

Sepsis caused by *S. aureus* and *E. coli*, but not by *S. pneumoniae*, shapes the TRD repertoire in young children

Zooming in on young children (<2 years) indicated that sepsis-related changes could be observed in the TRD repertoire according to the pathogen (Supporting Information Fig. S2). We, therefore, analyzed in more detail the characteristics of the TRD repertoire in young children (<2 years) infected by *E. coli*, *S. aureus*,

and *S. pneumoniae* and children of the same age who never had any invasive bacterial infection (Fig. 2; Table 1; Supporting Information Fig. S1B). In order to further minimize the potential effect of age on the TRD data within this age group, we analyzed in parallel the effect of pathogen (uninfected controls, *E. coli*, *S. aureus*, and *S. pneumoniae*) with age as a covariate using the analysis of covariance (ANCOVA; Supporting Information Table S1). The TRDV2 gene segment was used more commonly in children infected with *S. aureus* compared with uninfected children and children infected with *S. pneumoniae* or *E. coli* (Fig. 2A, left panel; Supporting Information Table S1) and associated with a lower number of N additions in the corresponding CDR3 (Fig. 2B, left panel; Supporting Information Table S1). Of note, TRDV2 usage and a corresponding number of N additions in the *E. coli* group were highly variable (Fig. 2A and B, left panels) and were inversely correlated (Fig. 2C). No difference in N additions was detected among TRDV1- and TRDV3-containing CDR3 (Fig. 2B, middle and right panel; Supporting Information Table S1), highlighting the specificity of the TRDV2 response. As the difference in N additions among TRDV2-containing CDR3 did not result in a difference in CDR3 length (Fig. 2D), we wondered whether differential TRDJ segment use could contribute to the minimization of the CDR3 length differences. Indeed, the TRDJ3 gene segment paired more commonly with the TRDV2 gene segment in the *S. aureus* group and, to a lesser extent, in the *E. coli* group than in the *S. pneumoniae* and control groups (Fig. 2E; Supporting Infor-

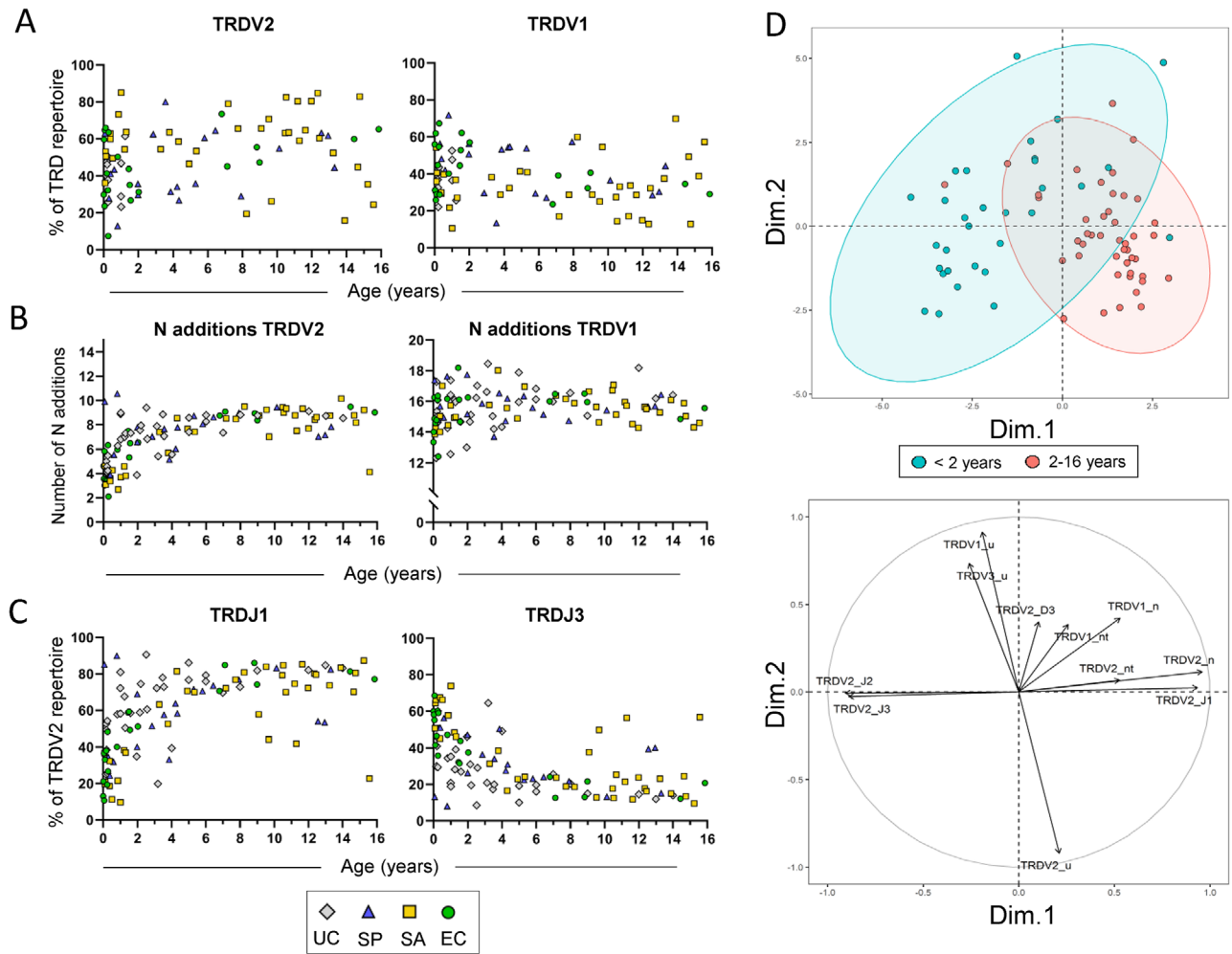


Figure 1. The TRD repertoire in children changes with age. (A) TRDV2 (left panel) and TRDV1 (right panel) usage by age. (B) Number of N additions from TRDV2- and TRDV1-containing CDR3 sequences by age. Each dot represents the weighted mean of an individual sample. (C) Percent frequency of TRDV2 sequences containing a TRDJ1 (left panel) or a TRDJ3 (right panel) segment by age. (D) Cumulative contribution of 11 parameters in a principal component analysis of the CDR3 δ repertoires by age (see Methods section for more details). Top: PCA with two-dimensional representation based on the first two principal components. Blue dots represent young children (<2 years, $n = 31$), and red dots represent older children (≥ 2 years, $n = 45$). Bottom: arrows indicate the projection of each original variable onto these principal components. The length of each arrow indicates the magnitude of contribution to the explained variance. Variables are labeled at the tip of each arrow for identification (TRDV2_D3 = % of TRDV2 sequences containing TRDD3; TRDV2_J1, TRDV2_J2, TRDV2_J3 = % of TRDV2 sequences containing TRDJ1 or TRDJ2 or TRDJ3; TRDV1_u, TRDV2_u, TRDV3_u = % of TRDV1 usage, % of TRDV2 usage, % of TRDV3 usage (of total TRD); TRDV1_n, TRDV2_n = mean number of N additions in TRDV1 or TRDV2 sequences; TRDV1_nt, TRDV2_nt = mean CDR3 nucleotide length in TRDV1 or TRDV2 sequences). UC, uninfected control ($n = 10$ in A and $n = 33$ in B, C); SP, *S. pneumoniae* ($n = 20$ in A–C); SA, *S. aureus* ($n = 36$ in A–C); EC, *E. coli* ($n = 20$ in A–C). Uninfected control samples were obtained from datasets available in the public domain (see Materials and methods section for more details). Each dot represents a distinct biological replicate.

mation Table S1), likely explaining the observed CDR3 length conservation, given that TRDJ3 contains eight more nucleotides than TRDJ1 [29]. When following the pattern of N additions and TRDJ1/TRDJ3 usage with increasing age in the <2-year-old children, it can be seen that, in contrast to the other groups, these remain stable in the *S. aureus* group (Supporting Information Fig. S2). There was also an increase in the use of the TRDD3 gene segment (13 nucleotides) in the *S. aureus* group compared with the other groups at the expense of the shorter TRDD1 (8 nucleotides) and TRDD2 gene segments (9 nucleotides; Supporting Information Fig. S3A; Supporting Information Table S1). Note that the ANCOVA results (Supporting Information Table S1, post

hoc analyses with pairwise comparisons) confirm that the analyses performed by investigating the samples pooled per study group (Fig. 2) are not confounded by age.

To explore the possibility that specific infections might lead to the expansion of common CDR3 sequences, we investigated the level of sharing within the TRD repertoires associated with each pathogen. This analysis revealed strikingly increased sharing of the TRDV2 repertoire among young children (<2 years) infected with *S. aureus* compared with age-matched uninfected controls and children infected with *S. pneumoniae* or *E. coli* (Fig. 3A and B, left panel). The *E. coli* group showed an increase in TRDV2 sharing compared with *S. pneumoniae* and control groups (Fig. 3A

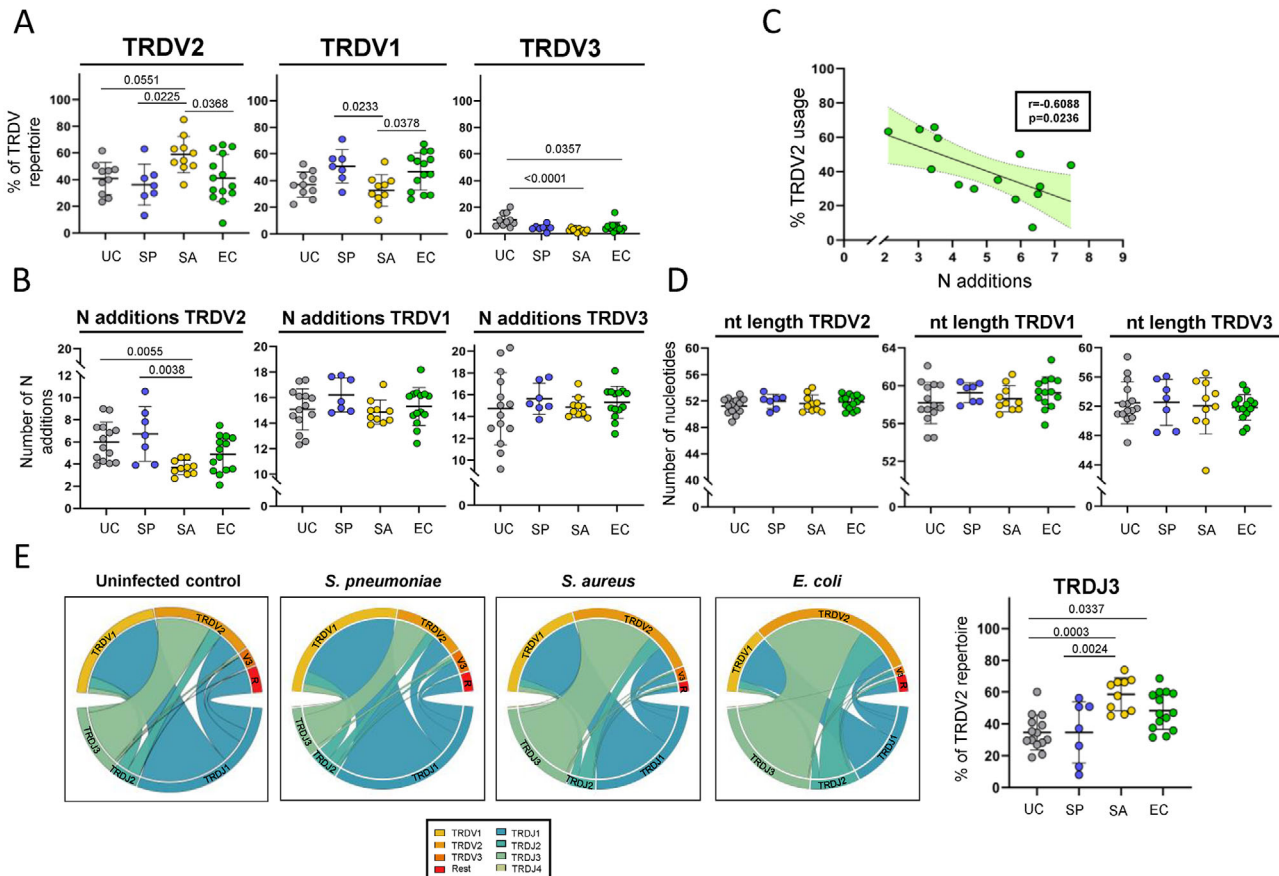


Figure 2. Sepsis induced by *S. aureus* or *E. coli* but not by *S. pneumoniae* shapes the TRD repertoire in young children. (A) Percent frequency of TRDV2-, TRDV1-, and TRDV3-containing CDR3 sequences from the TRD repertoires of (un)infected young children (<2 years). (B) Mean number of N additions (each dot represents the weighted mean of an individual sample) from TRDV2-, TRDV1-, and TRDV3-containing CDR3 sequences from the TRD repertoires of (un)infected young children (<2 years). (C) Mean number of TRDV2-containing CDR3 sequences and percent frequency of TRDV2-containing sequences from the TRD repertoires of young children (<2 years) infected with *E. coli*. (D) Mean nucleotide length of TRDV2-, TRDV1-, and TRDV3-containing CDR3 sequences from the TRD repertoires of (un)infected young children (<2 years). (E) Left: representative circoplots showing TRDV-TRDJ paired use in (un)infected young children (<2 years). The width of a link corresponds to the rearrangement frequency of a given V/J pairing. Right: percent frequency of sequences containing a TRDJ3 segment in the TRDV2 repertoires of young children (<2 years). (A, B, D, E) Data were analyzed using the Kruskal–Wallis test with Dunn’s multiple comparison test. Error bars indicate mean \pm SEM. (C) Data were analyzed using Spearman’s correlation. 95% confidence intervals are highlighted in light green. UC, uninfected control ($n = 10$ in A and $n = 14$ in B, D, E); SP, *S. pneumoniae* ($n = 7$ in A, B, D, E); SA, *S. aureus* ($n = 10$ in A, B, D, E); EC, *E. coli* ($n = 14$ in A–E). Each dot represents a distinct biological replicate.

and B, left panel). This increased TRDV2 sharing in the *S. aureus* and *E. coli* groups was independent of any associated increase in TRDV2 sequences with zero N additions or TRDV2 sequences paired with the TRDJ3 gene segment in the shared repertoire (Supporting Information Fig. S3B–D), consistent with increased sharing in both the TRDV2-TRDJ3 repertoire and the TRDV2-TRDJ1 repertoire (Fig. 3C). No increase in TRDV1 and TRDV3 sharing was observed in any of the bacterial infections studied here (Fig. 3B, middle and right panel), again highlighting the specificity of the TRDV2-containing $\gamma\delta$ TCR response against specific bacterial infections at this age.

Overall, the TRD repertoire in young children (<2 years) was profoundly shaped by invasive infection with *S. aureus* and, to a variable extent, with *E. coli*, whereas no such influence was observed following invasive infection with *S. pneumoniae*.

Shaping of the TRD repertoire by sepsis is specific for young children

Next, we quantified a series of TRD features in children aged less than two years and in children aged between two and 16 years to assess the influence of age at the time of infection (Fig. 4; Supporting Information Fig. S1B and C). Striking differences were observed as a function of age (<2 years versus 2–16 years) in the *S. aureus* and *E. coli* groups for sharing across the TRDV2 repertoire (Fig. 4A), N additions (Fig. 4B), and TRDJ use (Fig. 4C).

To extend this observation, we analyzed the TRD repertoire of adults with acute peritonitis [42]. Cases were stratified according to pathogen into infection with HMBPP-negative bacteria (that are not *S. aureus*), *S. aureus*, or HMBPP-positive bacteria (Fig. 4, Supporting Information Table S2). These adults displayed TRD repertoire characteristics that were essentially identical to those

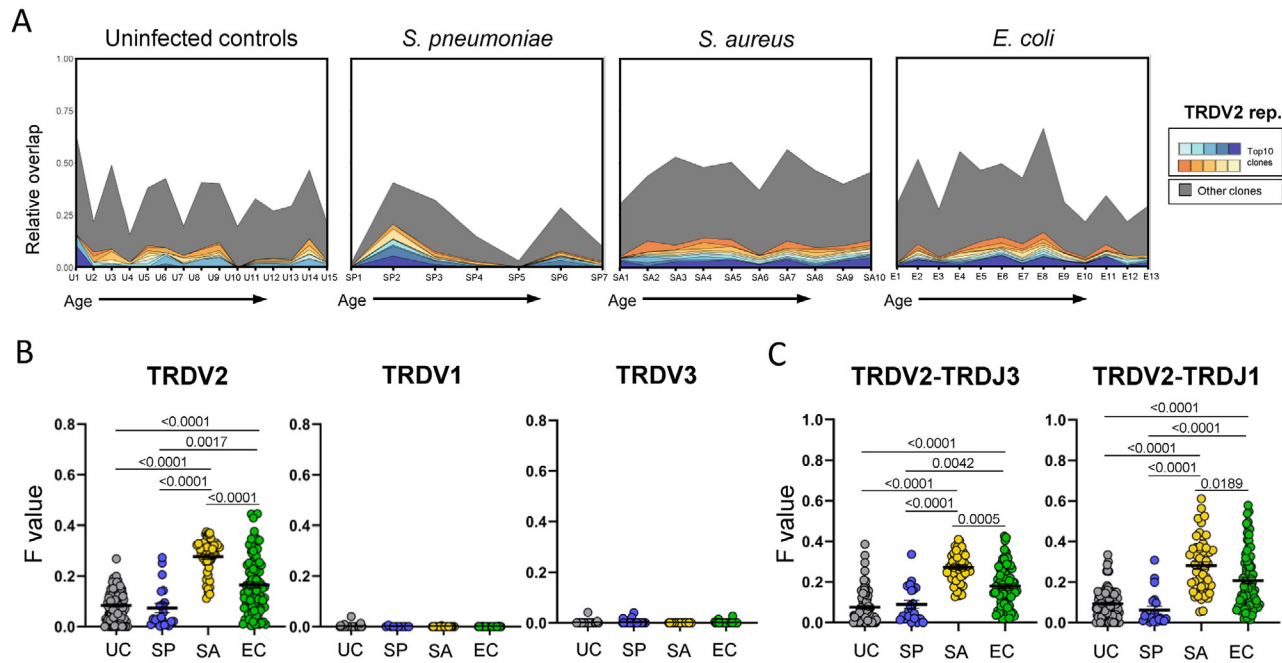


Figure 3. The TRDV2 repertoire of young children with *S. aureus* or *E. coli* sepsis is highly public. (A) Longitudinal tracking of shared TRDV2 sequences among young children (<2 years) by pathogen or uninfected controls. The frequencies of the top 10 most abundant shared clonotypes in each group are plotted in distinct colors, and the remaining fractions of shared TRDV2 sequences are plotted in dark grey at the top. Each tick on the X-axis corresponds to an individual in ascending order by age. The relative frequency of a particular sequence or group of sequences in the total TRDV2 repertoire of each individual is shown on the Y-axis. (B) Comparison of the geometric mean of relative overlap frequencies (F metrics by VDJ tools, see Methods for more details) between pairs of children infected with the same pathogen (or uninfected controls) for the TRDV2, TRDV1, and TRDV3 repertoires. (C) Comparison of the geometric mean of relative overlap frequencies (F metrics by VDJ tools) between pairs of children infected with the same pathogen (or uninfected controls) for the TRDV2-TRDJ1 and TRDV2-TRDJ3 repertoires. (B, C) Each dot represents the F value of a pair of samples. Data were analyzed using the Kruskal–Wallis test with Dunn’s multiple comparisons test. Error bars indicate mean \pm SEM. UC, uninfected control ($n = 14$ in B, C); SP, *S. pneumoniae* ($n = 7$ in B, C); SA, *S. aureus* ($n = 10$ in B, C); EC, *E. coli* ($n = 14$ in B, C).

observed in older children (≥ 2 years; Fig. 4), confirming the specificity of changes observed in the TRD repertoires of young children (<2 years) upon invasive bacterial infection with *S. aureus* or *E. coli*.

Shaping of the TRD repertoire in young children during invasive bacterial infection is due to expansion of a fetal TRD repertoire

Fetal and adult $V\gamma 9V\delta 2$ T cells develop distinctly, a process that is reflected in the TRD repertoire [29, 40]. As some of the TRD changes driven by *S. aureus* and, to a lesser extent, by *E. coli* (Fig. 2 and 3) were reminiscent of a fetal TRD repertoire (e.g. low numbers of N additions and frequent use of TRDJ3 and TRDD3), we compared the TRD repertoires from the different pathogen groups with fetal TRD repertoires (<30 weeks gestation). This analysis revealed that the blood TRD repertoires obtained from young children (<2 years) infected with *S. aureus* were shared to a greater extent with the fetal blood $V\gamma 9V\delta 2$ TRD repertoires than the blood TRD repertoires obtained from age-matched uninfected children and young children (<2 years) infected with *S. pneumoniae* (Fig. 5A and B). Relatively high numbers of overlap-

ping clonotypes rather than just a few abundant fetal clonotypes were responsible for this shared landscape (Fig. 5A–C). Again, the *E. coli* group showed a more variable degree of sharing with borderline significance compared with the *S. pneumoniae* and control groups (Fig. 5B and C). Accordingly, fetal $V\gamma 9V\delta 2$ T cells appeared to be highly responsive to invasive bacterial infection, especially with *S. aureus*, resulting in a restructuring of the TRD repertoire in young children (<2 years).

Discussion

In this study, we show that in early childhood (<2 years) but not in older children and adults, fetal-derived $V\gamma 9V\delta 2$ TCR clonotypes expand following invasive bacterial infections and that they do this in a pathogen-dependent manner.

$V\gamma 9V\delta 2$ T cells derived from <30 weeks gestation fetal blood [43], peripheral blood from preterm newborns [44], umbilical cord blood from full-term newborns [15, 45, 46], or peripheral blood from infants aged 10 weeks [40] react poorly in vitro against phosphoantigens including HMBPP. This relative lack of reactivity may be due to specific regulatory mechanisms that predominate in early life, such as those mediated by the inhibitory

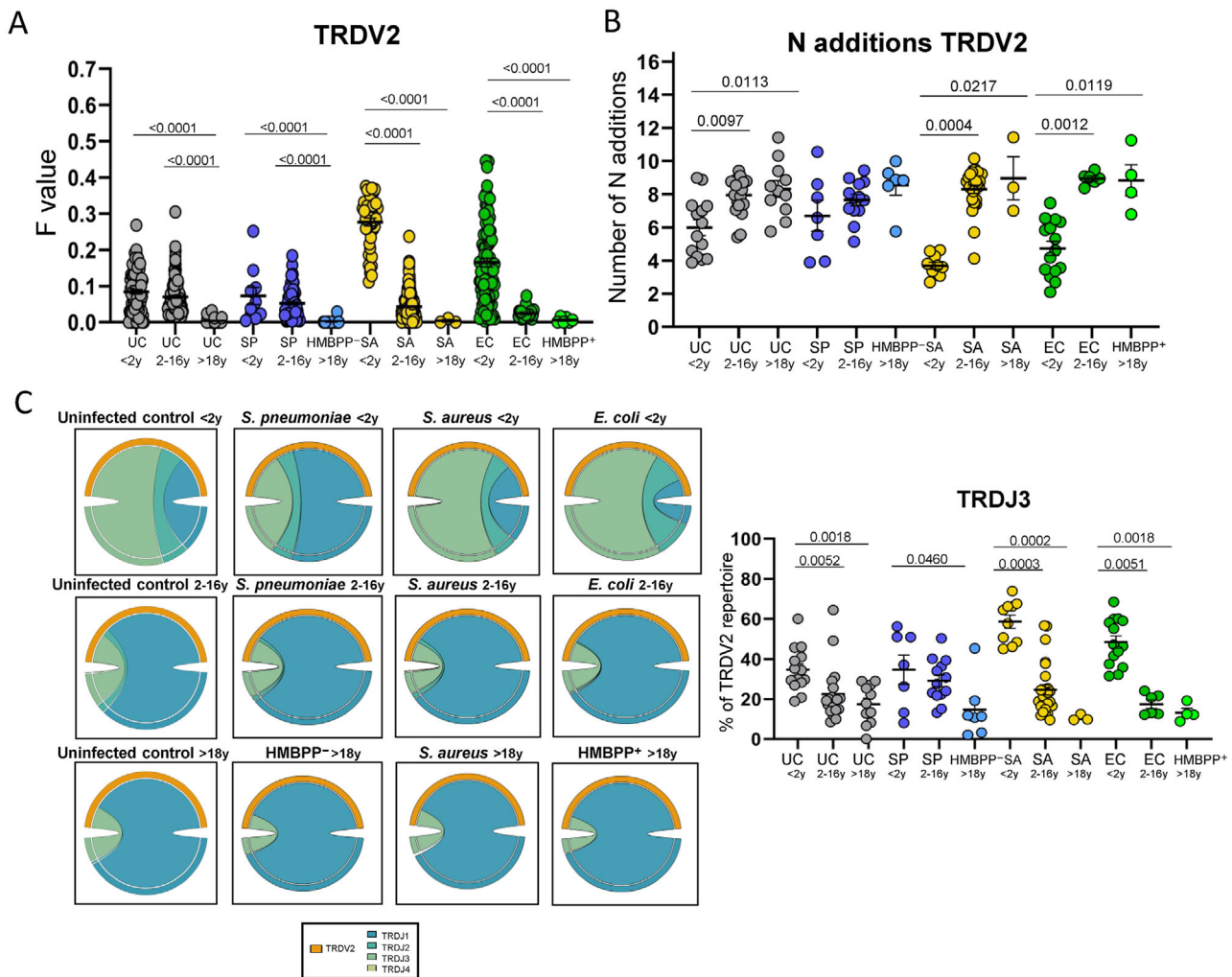


Figure 4. TRD repertoire shaping by sepsis is specific for young children. (A) Overlap frequencies (F metrics by VDJ tools) for the TRDV2 repertoire between pairs of uninfected and infected individuals belonging to the same study group (young children (<2 years), older children (≥2, between 2 and 16 years), and adults (>18 years)). (B) Mean number of N additions (each dot represents the weighted mean of an individual sample) for TRDV2-containing CDR3 sequences from the TRD repertoires of the different study groups. (C) Left: representative circoplots showing TRDV2-TRDJ paired use according to age. The width of a link corresponds to the rearrangement frequency of a given V/J pairing. Right: percent frequency of sequences containing a TRDJ3 segment in the TRDV2 repertoires according to age. (A–C) Data were analyzed using the Kruskal–Wallis test with Dunn’s multiple comparisons test. Error bars indicate mean ± SEM. UC, uninfected control; SP, *S. pneumoniae*; SA, *S. aureus*; EC, *E. coli*; HMBPP⁻, pathogens negative for HMBPP; HMBPP⁺, pathogens positive for HMBPP. In B and C, each dot represents a distinct biological replicate. In A–C, the number of samples in the distinct groups is UC = 14, SP = 7, SA = 10, EC = 14 in less than 2 years, UC = 18, SP = 13, SA = 26, EC = 6 in 2–16 years, and UC = 11, HMBPP⁻ = 7, SA = 3, HMBPP⁺ = 4 in >18 years.

receptor PD1 [47], which are thought to prevent harmful activation of cytotoxic and Th1-biased V γ 9V δ 2 T-cell responses in the developing fetuses and young children. These features are likely related to (tolerance) requirements of the fetal immune system, which involves a distinct thymic development [26, 29, 37]. Here we show that invasive bacterial infection with *S. aureus* or *E. coli* alters the TRD repertoire of V γ 9V δ 2 T cells in young children (<2 years) indicating that they respond to these pathogens. We further propose that such reshaping of the TRD repertoire in vivo reflects conditions that allow V γ 9V δ 2 T cells to bypass immunological tolerance [46, 48]. In addition, we found that fetal-derived V γ 9V δ 2 T-cell clonotypes expand preferentially during invasive bacterial

infection, consistent with the expression of high-affinity TCRs. The demonstration of such differential affinity between fetal and adult V γ 9V δ 2 T-cell clonotypes [29] is complicated because there is no clearly defined ligand structure for the CDR3 loops of the V γ 9V δ 2 TCRs [13, 49, 50]. In premature infants, sepsis has been associated with increased frequencies of $\gamma\delta$ T cells, albeit without the identification of a responsive subset at the level of V δ 1 versus V δ 2 TCRs [23]. Although V δ 1 T cells are abundant in cord blood and expand numerically in adults with sepsis [51], our data suggest that V δ 1 T cells do not react in young children with invasive bacterial infection and that reactivity within the $\gamma\delta$ T-cell compartment is driven mainly by fetal V γ 9V δ 2 T cells early after birth. We

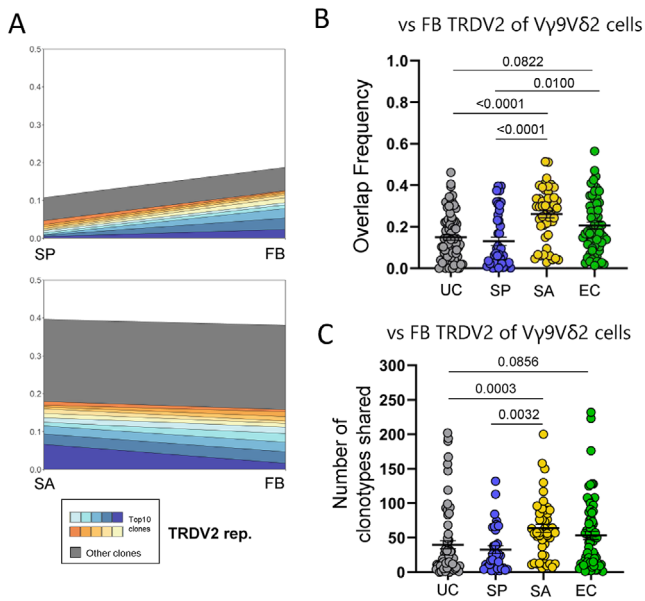


Figure 5. Sepsis induced by *S. aureus* or *E. coli* but not by *S. pneumoniae* results in the expansion of a fetal TRD repertoire in young children. (A) Representative shared clonotype abundance plots for TRDV2 repertoires in young children (<2 years) infected with SP or SA versus one fetal TRDV2 repertoire from flow-sorted V γ 9V δ 2 T cells. The frequencies of the top 10 most abundant shared clonotypes are plotted at the bottom in distinct colors, and the remaining fractions of shared TRDV2 sequences are plotted in dark grey at the top. (B) Relative abundance of the TRDV2 repertoires in young children (<2 years) infected with different pathogens (or uninfected controls) overlapping with the TRDV2 repertoire of flow-sorted fetal V γ 9V δ 2 T cells. Each dot represents a pair comparison. (C) Number of clonotypes shared between the TRDV2 repertoires of young children (<2 years) and the TRDV2 repertoire of flow-sorted fetal V γ 9V δ 2 T cells. Each dot represents a pair comparison. (B, C) Data were analyzed using the Kruskal–Wallis test with Dunn’s multiple comparisons test. Error bars indicate mean \pm SEM. UC, uninfected control ($n = 14$ in B, C); SP, *S. pneumoniae* ($n = 7$ in B, C); SA, *S. aureus* ($n = 10$ in B, C); EC, *E. coli* ($n = 14$ in B, C).

propose that postnatal thymic production [29, 52] is the source of most V γ 9V δ 2 T cells in the periphery after 2 years of age and that fetal thymus-derived V γ 9V δ 2 T cells become too dilute to expand appreciably in response to bacterial infection. In contrast, the V γ 9V δ 2 repertoire in premature infants is likely constituted primarily by fetal thymus-derived V γ 9V δ 2 T cells [26, 29], indicating that V γ 9V δ 2 T cells at this developmental stage may be highly responsive to systemic bacterial infection.

The well-annotated cohort of children with microbiologically documented bloodstream infection in the Swiss Pediatric Sepsis Study (SPSS) allowed us to determine the influence of pathogen type on the repertoire of V γ 9V δ 2 TCRs. HMBPP, a metabolite from the MEP pathway (also known as the nonmevalonate pathway) of isoprenoid synthesis in certain bacteria and parasites, is the most potent natural phosphoantigen [12, 14, 53]. Indeed, HMBPP activates V γ 9V δ 2 T cells approximately 10,000 times more efficiently than the ubiquitous phosphoantigen IPP, providing an innate-like signal of infection to the immune system [12, 14, 54]. As such, it was unexpected that the most robust V γ 9V δ 2 T-cell response,

at least as quantified in molecular terms, was observed in children infected with HMBPP-negative *S. aureus* rather than with HMBPP-positive *E. coli*. The reasons for this observation remain obscure. The superantigen staphylococcal enterotoxin A (SEA), which is known to bind specific V β chains, can also bind the V γ 9 chain [55], potentially activating V γ 9V δ 2 T cells in a manner akin to human-derived BTN2A1 [56, 57]. However, the concentrations of SEA required to induce the proliferation of V γ 9-expressing $\gamma\delta$ T-cell clones were several orders of magnitude higher than those required to induce a response in $\alpha\beta$ T-cell clones, questioning the relevance of this observation in vivo [55]. More recently, it has been suggested that V γ 9V δ 2 T cells can recognize *S. aureus*-infected dendritic cells, at least in part via the expressed TCR [58]. Of note, fetal-like TRD expansions (mouse TRDV4 [9]) have also been observed in a murine model of *S. aureus* skin infection, where they were associated with protection [59]. Accordingly, despite the lack of homology between the TRD repertoires in humans and mice [9, 33], a public/fetal-like TRD response against *S. aureus* infection appears to be a conserved mechanism across species in mammalian evolution. Our observations regarding fetal-derived V γ 9V δ 2 T-cell expansions in the *S. aureus* and *E. coli* groups are not explained by the presence of a single or a limited subset of TRDV2 sequences; instead, these expansions were polyclonal. While this observation may reflect an increased sensitivity of fetal TCR sequences toward specific pathogenic encounters, we cannot discount the possibility that this expansion is driven by specific (cytokine) stimuli from *E. coli* and *S. aureus* infections to which fetal-derived V γ 9V δ 2 T cells might be more sensitive. A similar phenomenon, where increased cytokine responsiveness rather than specific TCR engagement drives immune expansion, has also been described in early-life CD8 $^{+}$ $\alpha\beta$ T cells [60, 61].

This study has some limitations. Sampling from the SPSS was limited to blood RNA at a single time point. Therefore, we could not perform functional studies or investigate the time course of $\gamma\delta$ TCR repertoire changes. A very recent study found that both IFN γ^{+} and CD83 $^{+}$ V γ 9V δ 2 T cells were increased upon sepsis in a cohort of preterm infants, highlighting phenotypically diverse responses of fetal-derived V γ 9V δ 2 T cells upon bacterial infection [62]. As different pathogens affect different age groups [34], children infected by *S. pneumoniae*, *E. coli*, and *S. aureus* were not perfectly age-matched. To address this limitation, we performed an ANCOVA and included a control group of children <2 years who never had any invasive bacterial infection. The sample size did not allow to assess the impact of potential confounding factors, such as previous viral infections and comorbidities, on the $\gamma\delta$ TCR repertoire.

In summary, we have shown that young children (<2 years) but not older children and adults harbor fetal-derived V γ 9V δ 2 T cells that are highly responsive to specific bacterial pathogens in vivo. This finding challenges the idea that immune cells in early life are immature versions of their adult counterparts. We propose that fetal V γ 9V δ 2 T cells are held in check by various tolerance mechanisms, which are broken upon invasive infection with

specific pathogens unleashing their strong reactivity, at a time preceding the development of fully functional $\alpha\beta$ T-cell memory. This knowledge can guide further studies investigating the immune system in early childhood and potentially inform the development of new therapeutic approaches to improve the health of young children.

Materials and methods

Patients and samples

This multicenter study was based on a subset of the prospective observational SPSS [34]. Children aged between 0 and 16 years presenting with blood culture-proven bacterial sepsis were recruited in the ten major pediatric hospitals in Switzerland between September 2011 and December 2015. Sepsis was defined by the presence of positive blood cultures in children with a systemic inflammatory response syndrome, according to the 2005 pediatric consensus definition [63]. After having obtained written informed consent, we collected arterial or venous blood from the children. Whole arterial or venous blood was collected in PAXgene Blood RNA Tubes, which were subsequently cryopreserved at -80°C . The study was approved by Swissethics (KEK-029/11). Written informed consent was obtained in all cases in accordance with the principles of the Declaration of Helsinki.

Children infected with *E. coli*, *S. aureus*, or *S. pneumoniae* as the etiologic agent of sepsis were selected from the observational SPSS. Patients with conditions that might have influenced the number and/or the activation status of $\gamma\delta$ T cells, such as primary immune deficiency, systemic immunosuppression related to cancer therapy, autoimmune or inflammatory disease, transplantation, cystic fibrosis, and congenital infection with cytomegalovirus [18], were excluded from the study. High-throughput TRD sequencing data from healthy children who never had any invasive infection were obtained from previous studies: 10 children from Italy [19] and 24 children from Germany [64, 65, 66]. Fetal blood TRD repertoire data (5 samples, Belgium) were obtained similarly from a dataset available in the public domain [40].

V γ 9V δ 2 T cells were also isolated for TRD repertoire analysis from the peritoneal effluent of 14 dialysis patients presenting with acute peritonitis due to infection with either HMBPP-positive or HMBPP-negative bacteria, as listed in Supporting Information Table S2. The recruitment of peritoneal dialysis patients was approved by the South East Wales Local Ethics Committee (04WSE04/27), and the study was registered with the UK Clinical Research Network Study Portfolio (#11838, PERIT-PD). Patients with acute peritonitis (day 1) were admitted to the University Hospital of Wales. The diagnosis of acute peritonitis was based on the presence of abdominal pain and cloudy peritoneal effluent with >100 white blood cells/ mm^3 and a positive microbiological culture. Written informed consent was obtained from all participants in accordance with the principles of the Declaration

of Helsinki. High-throughput TRD sequencing data from V γ 9V δ 2 T cells of 11 healthy adult volunteers (8 adults from Belgium and 3 from South Africa) were obtained from a previous study [40].

RNA isolation and high-throughput sequencing

RNA was extracted from PAXgene Blood RNA Tubes (SPSS) using a PAXgene Blood RNA Kit (PreAnalytiX). The eluted RNA was subsequently concentrated to a volume of 14 μL volume using an RNeasy MinElute Cleanup Kit (Qiagen). This concentrated RNA was prepared for downstream TCR amplification. As functional TCR- γ rearrangements can be found in all peripheral blood T cells [67], we focused our analysis on TCR- δ chains, given the unseparated nature of our starting template. cDNA synthesis was conducted through a template-switch anchored reverse-transcription PCR. This employed a primer specific to the human constant delta gene segment (TRDC) with the sequence 5'-GTAGAATTCCTTACCAGACAAG-3', a template-switch adaptor with the sequence 5'-AAGCAGTGGTATCAACGCA-GAGTACATrGrG-3', and SuperScript II reverse transcriptase (Thermo Fisher Scientific). The cDNA was then purified using AMPure XP Beads (Agencourt). Amplification of the TRD region was achieved using an additional PCR incorporating another TRDC-specific primer (5'-GTCTCGTGGGCTCGGAGATGTGTATAAGAGACAGACGGATGGTTTGGTATGAGGCTGACTTCT-3', adapter sequence italicized) and a primer complementary to the template-switch adaptor (5'-TCGTCGGCAGCGTCAGATGTGTATAAGAGACAGAAGCAGTGGTATCAACGCAG-3', (adapter sequence italicized) in combination with a KAPA real-time library amplification kit (Kapa Biosystems). Amplification products were purified using AMPure XP Beads (Agencourt) and subjected to an index PCR incorporating sequencing adapters in combination with a Nextera XT index kit (Illumina). The final products were purified again using AMPure XP Beads (Agencourt) and sequenced at the GIGA Center (University of Liege, Belgium) using an Illumina MiSeq platform with MiSeq v3 600 cycles kit (ref: MS-102-3003).

$\gamma\delta$ T cells were also sorted via flow cytometry from the cloudy effluent sampled from peritoneal dialysis patients presenting with acute peritonitis. Briefly, peripheral blood mononuclear cells were isolated from peritoneal dialysis fluid via density gradient centrifugation using Lymphoprep (Axis-Shield). Cells were then stained with the following reagents: anti-CD14-V500 (clone M5E2), anti-CD19-V500 (clone HIB19), anti-CCR7-PE-Cy7 (clone 3D12), and anti-V δ 2-PE (clone B6) from BD Biosciences; anti-CD4-PE-Cy5.5 (clone S3.5) and LIVE/DEAD Fixable Aqua from Thermo Fisher Scientific; anti-CD3-APC/Fire 750 (clone SK7), anti-CD8-BV711 (clone RPA-T8), anti-CD27-BV421 (clone M-T271), anti-CD45RA-PE-Dazzle 594 (clone HI100), anti-TCR $\gamma\delta$ -PE-Cy5 (clone B1), and anti-V α 7.2-BV605 (clone 3C10) from BioLegend; anti-CD161-APC (clone 191B8) from Miltenyi Biotec; and anti-CXCR3-FITC (clone 49801) from R&D Systems. Viable T cells expressing V δ 2 were identified in the CD3⁺ lineage and sorted into RNAlater (Thermo Fisher Scientific) using

a custom-built FACSaria II (BD Biosciences) equipped with FACS-Diva software version 8.0 (BD Biosciences). TCR sequencing was performed by iRepertoire (MiSeq v2 500 cycle flow cell).

TRD repertoire analysis

CDR3 sequences were extracted from raw FASTQ files after aligning the reads to reference V, D, and J genes from TRD loci in the GenBank database using the MiXCR software version 3.0.12 [68]. CDR3 reads were assembled using the “assemble” function, and TRDD segments were assigned using the “OcloneFactoryParameters.dParameters.absoluteMinScore = 10” option based on three consecutive nucleotides from the international ImMunoGeneTics information system [69]. CDR3 sequences were further analyzed using VDJtools software version 1.2.1 [70]. Out-of-frame sequences and nonfunctional TRD segments were excluded from the analysis. Note that the TRDV gene usage was not calculated for uninfected children from the Ravens cohort (2020) [64], because in that cohort specific primers for TRDV genes were used (multiplex PCR) which can potentially result in a different TRDV content compared with the unbiased approach using a primer targeting the template-switch adaptor as in the current study; for other TRD sequencing read-outs, this has no potential influence. *F*-values representing the geometric mean of relative overlap frequencies between a pair of samples were calculated using the “CalcPairwiseDistances” function. PCA was performed using FactoMineR version 2.7 in R [71] with the following variables: % of TRDV2-TRDD3-containing sequences, % of TRDV2-TRDJ1-containing sequences, % of TRDV2-TRDJ2-containing sequences, % of TRDV2-TRDJ3-containing sequences, % of TRDV1 use, % of TRDV2 use, % of TRDV3 use, mean number of N additions in TRDV1 sequences, mean number of N additions in TRDV2 sequences, mean nucleotide length in TRDV1 sequences, and mean nucleotide length in TRDV2 sequences. All variables were scaled to a similar range using Z-score normalization prior to PCA. Results were visualized using FactoExtra version 1.0.7 in R. Circplots were generated using circlize version 0.4.15 in R [72].

Statistics

All statistical analyses except the ANCOVA were performed using Prism version 8.0.2 (GraphPad). To control for the effect of age on the different TCR repertoire variables in children aged under 2 years, we conducted an ANCOVA using the *rstatix* (v0.7.2) and *emmeans* (v1.10.0) R packages. We verified that the assumptions of the model (normality of residuals, homogeneity of variances, linearity) were met. Subsequently, we fitted the model and performed pairwise comparisons between groups using estimated marginal means. The results of the analysis (ANCOVA table, pairwise comparisons, and means of dependent variables before and after covariate adjustment) are presented in Supporting Information Table S1.

Acknowledgements: The authors thank Sarina Ravens and Alexa Cramer (Hannover Medical School, Germany) for sharing TRD FASTQ sequencing files from children without sepsis from their preliminary report on Research Square [65]. This work was supported by a WELBIO investigator program (WELBIO-CR-2022 A–15, DV), the Fonds De La Recherche Scientifique (FNRS, J.0225.20) (DV), the Fondation Jaumotte-Demoulin (DV), a Medical Research Council grant (MR/N023145/1, ME), a privileged partnership grant from the University of Lausanne and the ULB (DV, EG), the Swiss National Science Foundation (grant # 197618 to EG, 342730_153158/1 and 320030_201060/1 to Luregn Schlapbach), and the WEGH Foundation (to EG). G. Sanchez Sanchez (Télévie), M. Papadopoulou (post-doctoral fellowship), and I. Verdebout (aspirant) are supported by the FNRS. We thank the members of the Swiss Pediatric Sepsis Study (in alphabetical order): Christoph Aebi, Philipp K. A. Agyeman, Walter Bär, Christoph Berger, Sara Bernhard-Stirnemann, Eric Giannoni, Paul Hasters, Ulrich Heining, Christian R. Kahlert, Gabriel Konetzny, Antonio Leone, Giancarlo Natalucci, Anita Niederer-Loher, Klara M. Posfay-Barbe, Christa Relly, Thomas Riedel, Luregn J. Schlapbach, and Martin Stocker.

Conflict of interest: The authors declare no commercial or financial conflict of interest.

Author contributions: Eric Giannoni, David A. Price, Matthias Eberl, Luregn J. Schlapbach, and David Vermijlen conceived and supervised the study. Eric Giannoni, Philipp K.A. Agyeman, Donald J. Fraser, and Luregn J. Schlapbach led patient recruitment and acquisition of clinical data. Guillem Sanchez Sanchez, Eric Giannoni, Isoline Verdebout, Maria Papadopoulou, Moosa Rezwani, Raya Ahmed, Kristin Ladell, Kelly L. Miners, and James E. McLaren designed and performed the experiments; Guillem Sanchez Sanchez, Eric Giannoni, and David Vermijlen analyzed and interpreted the data. Eric Giannoni, Matthias Eberl, and Luregn J. Schlapbach acquired funding. Eric Giannoni, Guillem Sanchez Sanchez, and David Vermijlen wrote and revised the manuscript. All coauthors reviewed and revised the manuscript.

Data availability statement: FASTQ files of TRD sequences are deposited in the Sequence Read Archive (SRA) under accession no. PRJNA1033066.

Peer review: The peer review history for this article is available at <https://publons.com/publon/10.1002/eji.202451190>.

References

- Rudd, K. E., Johnson, S. C., Agesa, K. M., Shackelford, K. A., Tsoi, D., Kievlan, D. R., Colombara, D. V., et al., Global, regional, and national sep-

- sis incidence and mortality, 1990–2017: analysis for the Global Burden of Disease Study. *Lancet* 2020. **395**: 200–211.
- 2 Kollmann, T. R., Kampmann, B., Mazmanian, S. K., Marchant, A. and Levy, O., Protecting the newborn and young infant from infectious diseases: lessons from immune ontogeny. *Immunity* 2017. **46**: 350–363.
 - 3 Kollmann, T. R., Marchant, A. and Way, S. S., Vaccination strategies to enhance immunity in neonates. *Science* 2020. **368**: 612–615.
 - 4 Rudd, B. D., Neonatal T cells: a reinterpretation. *Annu. Rev. Immunol.* 2020. **38**: 229–247.
 - 5 Hayday, A. C., Integrative Immunology: Gamma Delta T Cells. In *Paul's fundamental immunology* 1748, Wolters Kluwer, 2022
 - 6 Vermijlen, D., Gatti, D., Kouzeli, A., Rus, T. and Eberl, M., $\gamma\delta$ T cell responses: How many ligands will it take till we know? *Semin. Cell Dev. Biol.* 2018. **84**: 75–86.
 - 7 Boehme, L., Roels, J. and Taghon, T., Development of $\gamma\delta$ T cells in the thymus – a human perspective. *Semin. Immunol.* 2022. **61–64**: 101662.
 - 8 Sanchez Sanchez, G., Tafesse, Y., Papadopoulou, M. and Vermijlen, D., Surfing on the waves of the human $\gamma\delta$ T cell ontogenic sea. *Immunol. Rev.* 2023. **315**: 89–107.
 - 9 Papadopoulou, M., Sanchez Sanchez, G. and Vermijlen, D., Innate and adaptive $\gamma\delta$ T cells: how, when, and why. *Immunol. Rev.* 2020. **298**: 99–116.
 - 10 Willcox, C. R., Mohammed, F. and Willcox, B. E., The distinct MHC-unrestricted immunobiology of innate-like and adaptive-like human $\gamma\delta$ T cell subsets—nature's CAR-T cells. *Immunol. Rev.* 2020. **298**: 25–46.
 - 11 Von Borstel, A., Chevour, P., Arsovski, D., Krol, J. M. M., Howson, L. J., Berry, A. A., Day, C. L., et al., Repeated *Plasmodium falciparum* infection in humans drives the clonal expansion of an adaptive $\gamma\delta$ T cell repertoire. *Sci. Transl. Med.* 2021. **13**: eabe7430.
 - 12 Eberl, M., Hintz, M., Reichenberg, A., Kollas, A.-K., Wiesner, J. and Jomaa, H., Microbial isoprenoid biosynthesis and human gammadelta T cell activation. *FEBS Lett.* 2003. **544**: 4–10.
 - 13 Hsiao, C.-H. C., Nguyen, K., Jin, Y., Vinogradova, O. and Wiemer, A. J., Ligand-induced interactions between butyrophilin 2A1 and 3A1 internal domains in the HMBPP receptor complex. *Cell Chem. Biol.* 2022. **29**: 985–995.e5.
 - 14 Morita, C. T., Jin, C., Sarikonda, G. and Wang, H., Nonpeptide antigens, presentation mechanisms, and immunological memory of human Vgamma2Vdelta2 T cells: discriminating friend from foe through the recognition of prenyl pyrophosphate antigens. *Immunol. Rev.* 2007. **215**: 59–76.
 - 15 Fichtner, A. S., Ravens, S. and Prinz, I., Human $\gamma\delta$ TCR repertoires in health and disease. *Cells* 2020. **9**: 800.
 - 16 Ramsburg, E., Tigelaar, R., Craft, J. and Hayday, A., Age-dependent requirement for gammadelta T cells in the primary but not secondary protective immune response against an intestinal parasite. *J. Exp. Med.* 2003. **198**: 1403–1414.
 - 17 Gibbons, D. L., Haque, S. F. Y., Silberzahn, T., Hamilton, K., Langford, C., Ellis, P., Carr, R., et al., Neonates harbour highly active $\gamma\delta$ T cells with selective impairments in preterm infants. *Eur. J. Immunol.* 2009. **39**: 1794–1806.
 - 18 Vermijlen, D., Brouwer, M., Donner, C., Liesnard, C., Tackoen, M., Van Ryselberge, M., Twité, N., et al., Human cytomegalovirus elicits fetal $\gamma\delta$ T cell responses in utero. *J. Exp. Med.* 2010. **207**: 807–821.
 - 19 Ma, L., Papadopoulou, M., Taton, M., Genco, F., Marchant, A., Meroni, V. and Vermijlen, D., Effector V γ 9V δ 2 T cell response to congenital *Toxoplasma gondii* infection. *JCI Insight* 2021. **6**: e138066.
 - 20 Cairo, C., Longinaker, N., Cappelli, G., Leke, R. G. F., Ondo, M. M., Djokam, R., Fogako, J., et al., Cord blood V2V δ 2 T cells provide a molecular marker for the influence of pregnancy-associated malaria on neonatal immunity. *J. Infect. Dis.* 2014. **209**: 1653–1662.
 - 21 Jagannathan, P., Lutwama, F., Boyle, M. J., Nankya, F., Farrington, L. A., Mcintyre, T. I., Bowen, K., et al., V δ 2+ T cell response to malaria correlates with protection from infection but is attenuated with repeated exposure. *Sci. Rep.* 2017. **7**: 11487.
 - 22 Guo, X.-Z. J., Dash, P., Crawford, J. C., Allen, E. K., Zamora, A. E., Boyd, D. F., Duan, S., et al., Lung $\gamma\delta$ T cells mediate protective responses during neonatal influenza infection that are associated with type 2 immunity. *Immunity* 2018. **49**: 531–544.e6.
 - 23 Rahman Qazi, K., Jensen, G. B., Van Der Heiden, M., Björkander, S., Marchini, G., Jenmalm, M. C., Abrahamsson, T., et al., Extreme prematurity and sepsis strongly influence frequencies and functional characteristics of circulating $\gamma\delta$ T and natural killer cells. *Clin. Transl. Immunol.* 2021. **10**: e1294.
 - 24 Tuengel, J., Ranchal, S., Maslova, A., Aulakh, G., Papadopoulou, M., Drissler, S., Cai, B., et al., Characterization of adaptive-like $\gamma\delta$ T cells in Ugandan infants during primary cytomegalovirus infection. *Viruses* 2021. **13**: 1987.
 - 25 Chen, Y.-S., Chen, I.-B., Pham, G., Shao, T.-Y., Bangar, H., Way, S. S. and Haslam, D. B., IL-17-producing $\gamma\delta$ T cells protect against *Clostridium difficile* infection. *J Clin Invest.* 2020. **130**: 2377–2390.
 - 26 Sanchez Sanchez, G., Papadopoulou, M., Azouz, A., Tafesse, Y., Mishra, A., Chan, J. K. Y., Fan, Y., et al., Identification of distinct functional thymic programming of fetal and pediatric human $\gamma\delta$ thymocytes via single-cell analysis. *Nat. Commun.* 2022. **13**: 5842.
 - 27 Sanchez Sanchez, G., Emmrich, S., Georga, M., Papadaki, A., Kossida, S., Seluanov, A., Gorbunova, V., et al., Invariant $\gamma\delta$ TCR natural killer-like effector T cells in the naked mole-rat. *Nat. Commun.* 2024. **15**: 4248.
 - 28 Damani-Yokota, P., Gillespie, A., Pasman, Y., Merico, D., Connelley, T. K., Kaushik, A. and Baldwin, C. L., Bovine T cell receptors and $\gamma\delta$ WC1 co-receptor transcriptome analysis during the first month of life. *Dev. Comp. Immunol.* 2018. **88**: 190–199.
 - 29 Papadopoulou, M., Tieppo, P., MCGovern, N., Gosselin, F., Chan, J. K. Y., Goetgeluk, G., Dauby, N., et al., TCR sequencing reveals the distinct development of fetal and adult human V γ 9V δ 2 T cells. *J. Immunol.* 2019. **203**: 1468–1479.
 - 30 Andreu-Ballester, J. C., Tormo-Calandín, C., Garcia-Ballesteros, C., Pérez-Griera, J., Amigó, V., Almela-Quilis, A., Ruiz Del Castillo, J., et al., Association of $\gamma\delta$ T cells with disease severity and mortality in septic patients. *Clin Vaccine Immunol.* 2013. **20**: 738–746.
 - 31 Liao, X.-L., Feng, T., Zhang, J.-Q., Cao, X., Wu, Q.-H., Xie, Z.-C., Kang, Y., et al., Phenotypic changes and impaired function of peripheral $\gamma\delta$ T cells in patients with sepsis. *Shock* 2017. **48**: 321–328.
 - 32 Matsushima, A. Ogura, H., Fujita, K., Koh, T., Tanaka, H., Sumi, Y., Yoshiya, K., et al., Early activation of $\gamma\delta$ T lymphocytes in patients with severe systemic inflammatory response syndrome. *Shock* 2004. **22**: 11–15.
 - 33 Herrmann, T., Karunakaran, M. M. and Fichtner, A. S., A glance over the fence: using phylogeny and species comparison for a better understanding of antigen recognition by human $\gamma\delta$ T-cells. *Immunol. Rev.* 2020. **298**: 218–236.
 - 34 Agyeman, P. K. A., Schlapbach, L. J., Giannoni, E., Stocker, M., Posfay-Barbe, K. M., Heininger, U., Schindler, M., et al., Epidemiology of blood culture-proven bacterial sepsis in children in Switzerland: a population-based cohort study. *Lancet Child Adolesc. Health* 2017. **1**: 124–133.
 - 35 GBD 2019 Antimicrobial Resistance Collaborators. Global mortality associated with 33 bacterial pathogens in 2019: a systematic analysis for the Global Burden of Disease Study 2019. *Lancet* 2022. **400**: 2221–2248.

- 36 Olin, A., Henckel, E., Chen, Y., Lakshminanth, T., Pou, C., Mikes, J., Gustafsson, A., et al., Stereotypic immune system development in newborn children. *Cell* 2018. **174**: 1277–1292.e14.
- 37 Rackaityte, E. and Halkias, J., Mechanisms of fetal T cell tolerance and immune regulation. *Front. Immunol.* 2020. **11**: 588.
- 38 Tabilas, C., Iu, D. S., Daly, C. W. P., Yee Mon, K. J., Reynaldi, A., Wesnak, S. P., Grenier, J. K., et al., Early microbial exposure shapes adult immunity by altering CD8+ T cell development. *Proc. Natl. Acad. Sci.* 2022. **119**: e2212548119.
- 39 Dorshkind, K. and Crooks, G., Layered immune system development in mice and humans. *Immunol. Rev.* 2023. **315**: 5–10.
- 40 Papadopoulou, M., Dimova, T., Shey, M., Briel, L., Veldtsman, H., Khomba, N., Africa, H., et al., Fetal public V γ 9V δ 2 T cells expand and gain potent cytotoxic functions early after birth. *Proceedings of the National Academy of Sciences of the United States of America* 2020. **117**: 18638–18648.
- 41 Davey, M. S., Willcox, C. R., Hunter, S., Kasatskaya, S. A., Remmerswaal, E. B. M., Salim, M., Mohammed, F., et al., The human V δ 2+ T-cell compartment comprises distinct innate-like V γ 9+ and adaptive V γ 9- subsets. *Nat. Commun.* 2018. **9**: 1760.
- 42 Liuzzi, A. R., Kift-Morgan, A., Lopez-Anton, M., Friberg, I. M., Zhang, J., Brook, A. C., Roberts, G. W., et al., Unconventional human T cells accumulate at the site of infection in response to microbial ligands and induce local tissue remodeling. *J. Immunol.* 2016. **197**: 2195–2207.
- 43 Dimova, T., Brouwer, M., Gosselin, F., Tassignon, J., Leo, O., Donner, C., Marchant, A., et al., Effector v γ 9v δ 2 t cells dominate the human fetal $\gamma\delta$ t-cell repertoire. *Proceedings of the National Academy of Sciences of the United States of America* 2015. **112**: E556–E565.
- 44 Van Der Heiden, M., Björkander, S., Rahman Qazi, K., Bittmann, J., Hell, L., Jenmalm, M. C., Marchini, G., et al., Characterization of the $\gamma\delta$ T-cell compartment during infancy reveals clear differences between the early neonatal period and 2 years of age. *Immunol. Cell Biol.* 2020. **98**: 79–87.
- 45 Cairo, C., Mancino, G., Cappelli, G., Pauza, C. D., Galli, E., Brunetti, E. and Colizzi, V., V δ 2 T-lymphocyte responses in cord blood samples from Italy and Côte d'Ivoire. *Immunology* 2008. **124**: 380–387.
- 46 Moens, E., Brouwer, M., Dimova, T., Goldman, M., Willems, F. and Vermijlen, D., IL-23R and TCR signaling drives the generation of neonatal V 9V 2 T cells expressing high levels of cytotoxic mediators and producing IFN- and IL-17. *J. Leukocyte Biol.* 2011. **89**: 743–752.
- 47 Hsu, H., Boudova, S., Mvula, G., Divala, T. H., Mungwira, R. G., Harman, C., Laufer, M. K., et al., Prolonged PD1 expression on neonatal V δ 2 lymphocytes dampens proinflammatory responses: role of epigenetic regulation. *J. Immunol.* 2016. **197**: 1884–1892.
- 48 Cairo, C., Sagnia, B., Cappelli, G., Colizzi, V., Leke, R. G. F., Leke, R. J. and Pauza, C. D., Human cord blood $\gamma\delta$ T cells expressing public V γ 2 chains dominate the response to bisphosphonate plus interleukin-15. *Immunology* 2013. **138**: 346–360.
- 49 Willcox, C. R., Salim, M., Begley, C. R., Karunakaran, M. M., Easton, E. J., Von Klotek, C., Berwick, K. A., et al., Phosphoantigen sensing combines TCR-dependent recognition of the BTN3A IgV domain and germline interaction with BTN2A1. *Cell Rep.* 2023. **42**: 112321.
- 50 Yuan, L., Ma, X., Yang, Y., Qu, Y., Li, X., Zhu, X., Ma, W., et al., Phosphoantigens glue butyrophilin 3A1 and 2A1 to activate V γ 9V δ 2 T cells. *Nature* 2023. **621**: 840–848.
- 51 Wang, X., Li, W., Zhu, D., Zhao, H., Chen, P. and Chen, X., Characterization of human peripheral blood $\gamma\delta$ T cells in patients with sepsis. *Exp. Ther. Med.* 2020. <https://doi.org/10.3892/etm.2020.8615>.
- 52 Perriman, L., Tavakolinia, N., Jalali, S., Li, S., Hickey, P. F., Amann-Zalcenstein, D., Ho, W. W. H., et al., A three-stage developmental pathway for human V γ 9V δ 2 T cells within the postnatal thymus. *Sci. Immunol.* 2023. **8**: eabo4365.
- 53 Liuzzi, A. R., McLaren, J. E., Price, D. A. and Eberl, M., Early innate responses to pathogens: pattern recognition by unconventional human T-cells. *Curr. Opin Immunol.* 2015. **36**: 31–37.
- 54 Shen, L., Frencher, J., Huang, D., Wang, W., Yang, E., Chen, C. Y., Zhang, Z., et al., Immunization of V γ 2V δ 2 T cells programs sustained effector memory responses that control tuberculosis in nonhuman primates. *Proc. Natl. Acad. Sci. USA* 2019. **116**: 6371–6378.
- 55 Morita, C. T., Li, H., Lamphear, J. G., Rich, R. R., Fraser, J. D., Mariuzza, R. A. and Lee, H. K., Superantigen recognition by gammadelta T cells: SEA recognition site for human Vgamma2 T cell receptors. *Immunity* 2001. **14**: 331–344.
- 56 Rigau, M., Ostrouska, S., Fulford, T. S., Johnson, D. N., Woods, K., Ruan, Z., McWilliam, H. E. G., et al., Butyrophilin 2A1 is essential for phosphoantigen reactivity by $\gamma\delta$ T cells. *Science* 2020. **367**: eaay5516.
- 57 Karunakaran, M. M., Willcox, C. R., Salim, M., Paletta, D., Fichtner, A. S., Noll, A., Starick, L., et al., Butyrophilin-2A1 directly binds germline-encoded regions of the V γ 9V δ 2 TCR and is essential for phosphoantigen sensing. *Immunity* 2020. **52**: 487–498.e6.
- 58 Cooper, A. J. R., Lalor, S. J. and Mcloughlin, R. M., Activation of human V δ 2+ $\gamma\delta$ T cells by staphylococcus aureus promotes enhanced anti-staphylococcal adaptive immunity. *J. Immunol.* 2020. **205**: 1039–1049.
- 59 Dillen, C. A., Pinsker, B. L., Marusina, A. I., Merleev, A. A., Farber, O. N., Liu, H., Archer, N. K., et al., Clonally expanded $\gamma\delta$ T cells protect against *Staphylococcus aureus* skin reinfection. *J. Clin. Invest.* 2018. **128**: 1026–1042.
- 60 Davenport, M. P., Smith, N. L. and Rudd, B. D., Building a T cell compartment: how immune cell development shapes function. *Nat Rev. Immunol.* 2020. **20**: 499–506.
- 61 Watson, N. B., Patel, R. K., Kean, C., Veazey, J., Oyesola, O. O., Laniewski, N., Grenier, J. K., et al., The gene regulatory basis of bystander activation in CD8+ T cells. *Sci. Immunol.* 2024. **9**: eadf8776.
- 62 León-Lara, X., Fichtner, A. S., Willers, M., Yang, T., Schaper, K., Riemann, L., Schöning, J., et al., $\gamma\delta$ T cell profiling in a cohort of preterm infants reveals elevated frequencies of CD83+ $\gamma\delta$ T cells in sepsis. *J. Exp. Med.* 2024. **221**: e20231987.
- 63 Goldstein, B., Giroir, B. and Randolph, A. and International Consensus Conference on Pediatric Sepsis. International pediatric sepsis consensus conference: definitions for sepsis and organ dysfunction in pediatrics. *Pediatr Crit Care Med.* 2005. **6**: 2–8.
- 64 Ravens, S., Fichtner, A. S., Willers, M., Torkomoo, D., Pirr, S., Schöning, J., Deseke, M., et al., Microbial exposure drives polyclonal expansion of innate $\gamma\delta$ T cells immediately after birth. *Proc. Natl. Acad. Sci.* 2020. **117**: 18649–18660.
- 65 Ravens, S., Cramer, A., Riemann, L., Almeida V., Yang, T., Kammeyer, C., Gluschke, E., et al., Early-life thymectomy enhances persistence of fetal-derived $\Gamma\delta$ T cells in children with congenital heart disease. 2023. <https://www.researchsquare.com/article/rs-3621915/v1>
- 66 Schlapbach, L. J., Watson, R. S., Sorce, L. R., Argent, A. C., Menon, Kusum, Hall, M. W. et al., International Consensus Criteria for Pediatric Sepsis and Septic Shock. *JAMA.* 2024. **331**(8): 665–674.
- 67 Sherwood, A. M., Desmarais, C., Livingston, R. J., Andriesen, J., Haussler, M., Carlson, C. S. and Robins, H., Deep sequencing of the human TCR γ and TCR β repertoires suggests that TCR β rearranges after $\alpha\beta$ and $\gamma\delta$ T cell commitment. *Sci. Transl. Med.* 2011. **3**: 90ra61.
- 68 Bolotin, D. A., Poslavsky, S., Mitrophanov, I., Shugay, M., Mamedov, I. Z., Putintseva, E. V. and Chudakov, D. M., MiXCR: software for comprehensive adaptive immunity profiling. *Nat Methods* 2015. **12**: 380–381.

- 69 Yousfi Monod, M., Giudicelli, V., Chaume, D. and Lefranc, M.-P., IMGT/JunctionAnalysis: the first tool for the analysis of the immunoglobulin and T cell receptor complex V-J and V-D-J JUNCTIONS. *Bioinformatics* 2004. 20: i379–385.
- 70 Shugay, M., Bagaev, D. V., Turchaninova, M. A., Bolotin, D. A., Britanova, O. V., Putintseva, E. V., Pogorelyy, M. V., et al., VDJtools: unifying post-analysis of T cell receptor repertoires. *PLoS Comput Biol* 2015. 11: e1004503.
- 71 Lê, S., Josse, J. and Husson, F., FactoMineR: an R package for multivariate analysis. *J. Stat. Softw.* 2008. 25: 1–18.
- 72 Gu, Z., Gu, L., Eils, R., Schlesner, M. and Brors, B., circlize implements and enhances circular visualization in R. *Bioinformatics* 2014. 30: 2811–2812.

Abbreviations: **CDR3:** complementarity determining region 3
· **HMBPP:** (E)-4-hydroxy-3-methyl-but-2-enyl pyrophosphate ·

MEP: 2-C-methyl-D-erythritol 4-phosphate · **PCA:** principal component analysis · **TCRs:** T-cell receptors · **TdT:** terminal deoxynucleotidyl transferase

Full correspondence: Prof. David Vermijlen, Department of Pharmacotherapy and Pharmaceutics, Université Libre de Bruxelles (ULB), Brussels, 1050 Belgium
e-mail: david.vermijlen@ulb.be

Received: 15/4/2024

Revised: 12/7/2024

Accepted: 16/7/2024

Accepted article online: 18/7/2024